Active Contours for Cell Tracking

Nilanjan Ray and Scott T. Acton
Department of Electrical and Computer Engineering,
University of Virginia, Charlottesville, VA 22904
{nray, acton}@virginia.edu

Abstract

This paper introduces an active contour or snake-based method for tracking cells within a video sequence. Specifically, we apply our cell tracking techniques to rolling leukocytes observed in vivo (in living animal) from video microscopy. The analysis of leukocyte motion reveals cues about the mechanism of inflammatory disease. To attack the problem of tracking leukocytes in vivo, the proposed snake tracker utilizes shape and size information specific to the leukocytes. The principal contribution of this work lies in introducing the shape and size constraint as a geometric primitive in the parametric snake energy model. The energy functional is then minimized through the basic principles of the calculus of variations to obtain the Euler equations used in contour updating. We have developed a partial differential equation (PDE) based generalized gradient vector flow (GVF) that accommodates for contrast changes and weak cell edges. Whereas previous GVF models are sensitive to initial contour placement, the modified GVF construction with Dirichlet type boundary condition (BC) allows a snake tracker to be robust for a wide range of initial positions. Another contribution in this work is to incorporate an energy term in the snake model that eliminates the need for explicitly resampling the snake contour intermittently as performed in traditional snake evolution. Using animal experiments, we compare the accuracy of the proposed snake tracker with the correlation and centroid based tracker and show that the proposed tracker is superior in terms of increased number of frames tracked and reduced localization error.

1. Introduction

Leukocyte tracking *in vivo* has gained its importance to the research groups studying inflammatory disease [1,2]. The analysis of leukocyte rolling is emerging as an important tool in potential and novel anti-inflammatory treatments. For example, E-selectin inhibitors are capable of decreasing the number and increasing the velocity of rolling leukocytes in living animals [3]. Presently, the analysis of rolling velocities is quite laborious requiring tens of hours of user-interactive image processing work for each experiment. In a single hour of experimentation, more than 100,000 frames of video data are produced. To manually inspect each frame for leukocyte position recording is next to impossible. Thus we seek automated leukocyte tracking methods to obtain leukocyte positions and to compute leukocyte velocities.

To meet such requirements, we propose a shape-size constrained active contour based tracker in this work. The associated energy has a constraint term that penalizes the deviation of the snake from a prescribed circular shape and size. To track fast rolling leukocytes, we also propose an enhancement of the GVF flow [4,5] through constraining Dirichlet BC. The improvements allow us to double the maximum speed of cells tracked from about 100 μm/s to 200 μm/s. Another contribution in this work is to eliminate the need for explicitly resampling the snake contour by introducing an energy functional in the snake model that keeps the neighboring snake points equally apart.

In the next section, we introduce the parametric active contour approach. Section 3 explains background for GVF. In section 4 we introduce the proposed enhanced GVF. Section 5 illustrates shape-size constraint on the snake followed by the implicit resampling in section 6. Section 7 shows the final snake model integrating enhanced GVF, shape-size and resampling constraint. In section 8 we discuss the results of tracking leukocytes *in vivo* with the proposed snake model and compare the same with two other standard methods – centroid [6] and correlation [7] based tracker.

2. Parametric Active Contours

A parametric active contour or snake is a curve, $\mathbf{C}(s)$ with parameter $s \in [0,1]$. The curve can move on the image plane under the influence of two types of forces – internal and the external forces. The former constrains the snake to be smooth while the latter guides the snake to seek desirable image properties, such as edges. The external forces are computed from the image data. Such an active contour model seeks to minimize the following functional [8]:

$$E_{\text{snake}} = \int_0^1 \frac{1}{2}\left\{\alpha\left|\mathbf{C}'(s)\right|^2 + \beta\left|\mathbf{C}''(s)\right|^2\right\} + E_{\text{ext}}\left[\mathbf{C}(s)\right] ds, \quad (1)$$

where the first bracketed energy term defines the internal energy of the snake. The non-negative constants α and β

Fifth IEEE Southwest Symposium on Image Analysis and Interpretation (SSIAI'02)
0-7695-1537-1/02 $17.00 © 2002 IEEE

are the resistance to stretching and bending of the active contour, respectively. The external energy term E_{ext} is usually defined as $-|\nabla G_\sigma(x,y) * I(x,y)|$ [8], where $I(x,y)$ is the image intensity at (x,y), $G_\sigma(x,y)$ is a 2D Gaussian kernel with standard deviation σ. Calculus of variations [9] is applied to minimize (1) to obtain the following Euler or the motion equations [8]:

$$\alpha\mathbf{C}''(s) - \beta\mathbf{C}''''(s) - \nabla E_{ext}(\mathbf{C}(s)) = 0. \quad (2)$$

The Euler equations (2) are called snake evolution equations and can be essentially viewed as a force balance equation, where $-\nabla E_{ext}$ can be thought of as an external force (u,v) [4]. Then (2) takes the general form of force balance equations:

$$\alpha\mathbf{C}''(s) - \beta\mathbf{C}''''(s) + (u(\mathbf{C}(s)), v(\mathbf{C}(s))) = 0. \quad (3)$$

In this paper, (u, v) is a GVF force.

3. Gradient Vector Flow

The gradient vector flow field $(u(x,y), v(x,y))$ is derived from the following energy functional in [4,5]:

$$E_{\text{GVF}}(u,v) = \frac{1}{2}\iint g(|\nabla f|)\left(u_x^2 + u_y^2 + v_x^2 + v_y^2\right)dxdy + \frac{1}{2}\iint (1 - g(|\nabla f|))((u - f_x)^2 + (v - f_y)^2)dxdy. \quad (4)$$

In this context, f is the edge map, and g is a decreasing function of the gradient magnitude defined as [4,5]:

$$f(x,y) = |\nabla G_\sigma(x,y) * I(x,y)|, \quad (5)$$

$$g(|\nabla f|) = \exp(-(\frac{|\nabla f|}{K})). \quad (6)$$

K is a positive constant controlling the smoothness of the resulting field [4,5]. Calculus of variations is once again applied to Minimize (4) leading to the following Euler equations [5]:

$$g\nabla^2 u - (1-g)(u - f_x) = 0,$$
$$g\nabla^2 v - (1-g)(v - f_y) = 0. \quad (7)$$

One solves (7) to obtain the GVF force field (u,v) that minimizes (4).

4. Constrained Gradient Vector Flow

In visual tracking with snakes an accepted strategy for snake initialization is as follows. After capturing the object in the current frame, take the position of this snake and place it on the next frame [10]. Following such a strategy with a GVF snake does not lead to capturing of leukocyte when the frame-to-frame cell displacement is high or equivalently the temporal resolution is low, since the standard GVF snake fails if the initial snake does not include the object medial axis [11]. One example is shown in Figure 1a. This deficiency leaves a scope to enhance the original GVF force towards making it robust to snake initialization. Thus we propose the snake-force (u,v), constraining the GVF-PDE's through Dirichlet BC's as follows:

$$\left.\begin{aligned} g\nabla^2 u - (1-g)(u - f_x) = 0 \\ g\nabla^2 v - (1-g)(v - f_y) = 0 \end{aligned}\right\} \text{when } (x,y) \in (D - C), \quad (8)$$

$$(u(x,y), v(x,y)) = \mathbf{v}, \text{ when } (x,y) \in \partial C \text{ and}$$
$$\nabla(u(x,y), v(x,y)) = \mathbf{0}, \text{ when } (x,y) \in \partial D, \quad (9)$$

where D is the rectangular image domain with boundary ∂D and C is the region bounded by the initial closed snake with boundary ∂C, and $\mathbf{v}$ is the direction of the leukocyte movement. It is to be noted that the BC for the initial snake boundary ∂C is of Dirichlet type while that for the image boundary ∂D is Neumann type [12]. Since the latter one is the natural boundary condition [12] here, the only constraining BC is the Dirichlet one and is responsible for the proposed enhancement. Adding such a BC improves tracking the rolling leukocytes as Figure 1b demonstrates. In generating the result here, we use the prior knowledge about the direction of cell movement, *i.e.*, $\mathbf{v}$=(-1,0).

5. Shape-size Constraint

The principal contribution in this work is the design of an energy functional that constrains the snake size and shape in order to capture leukocytes. Here $\mathbf{x}$ denotes the ensemble of x-coordinates of all the snake (contour) points $\mathbf{C}(s)=(x(s),y(s))$, *i.e.*, $\mathbf{x}=[x(s)]^T$, $s \in [0,1]$; similarly, $\mathbf{y}$ denotes the y-coordinates of all the snake points, and K is the expected cell radius. The shape energy functional takes the form:

$$E_{\text{shape}}(\mathbf{x},\mathbf{y}) = \frac{1}{2}\int_0^1 \left(R_x(s,x(s)) - \bar{R}(\mathbf{x},\mathbf{y})\cos(2\pi s)\right)^2 ds + \frac{1}{2}\int_0^1 \left(R_y(s,y(s)) - \bar{R}(\mathbf{x},\mathbf{y})\sin(2\pi s)\right)^2 ds, \quad (10)$$

where $R_x(s,x(s))$, $R_y(s,y(s))$ and $\bar{R}(\mathbf{x},\mathbf{y})$ are defined as:

$$R_x(s,x(s)) = x(s) - \int_0^1 x(r)dr,$$
$$R_y(s,y(s)) = y(s) - \int_0^1 y(r)dr \text{ and}$$
$$\bar{R}(\mathbf{x},\mathbf{y}) = \int_0^1 \sqrt{R_x(s,x(s))^2 + R_y(s,y(s))^2}\,ds. \quad (11)$$

Similarly, the size constraint energy functional is as follows:

$$E_{\text{size}}(\mathbf{x},\mathbf{y}) = \frac{1}{2}\left(\bar{R}(\mathbf{x},\mathbf{y}) - K\right)^2. \quad (12)$$

Following the basic principles of the calculus of variations [9] and applying the du Bois lemma [13], we can show that the Euler equations that result from (10) and (12) are as follows:

$$x(s) - \int_0^1 x(r)dr - \bar{R}(\mathbf{x},\mathbf{y})\cos(2\pi s) = 0 \text{ and}$$
$$y(s) - \int_0^1 y(r)dr - \bar{R}(\mathbf{x},\mathbf{y})\sin(2\pi s) = 0, \quad (13)$$

and

$$\frac{(\bar{R}(\mathbf{x},\mathbf{y}) - K)(x(s) - \int_0^1 x(r)dr)}{\sqrt{R_x^2(s,x(s)) + R_y^2(s,y(s))}} = 0, \text{ and}$$
$$\frac{(\bar{R}(\mathbf{x},\mathbf{y}) - K)(y(s) - \int_0^1 y(r)dr)}{\sqrt{R_x^2(s,x(s)) + R_y^2(s,y(s))}} = 0. \quad (14)$$

The way we use these equations (13) and (14) in our snake computations is discussed in section 7.

6. Implicit Resampling

To approximate the entire continuous contour, a number of points from the contour are chosen. These points are sometimes referred to as *snaxels*. The continuous parameter *s* used so far to denote the snaxel position ($x(s)$, $y(s)$) is indexed now by $i \in \{0,1,\ldots n\text{-}1\}$, with *n* being the total number of snaxels in the snake. So, we have a discrete contour point or snaxel as (x_i, y_i). In vector notation we write the snaxels collectively as (**x**, **y**), where this time for the discrete version, $\mathbf{x}=[x_0,\ldots x_{n-1}]^T$ and $\mathbf{y}=[y_0,\ldots y_{n-1}]^T$. In general, during the snake evolution, some portion of the snake will be stretched while the other portion will be shortened. These compression and rarefaction require a resampling of the contour under evolution. The resampling is usually done explicitly by choosing sample points uniformly during the snake evolution [4]. The cost of such explicit sampling is O(*n*), for a total of *n* snaxels.

To maintain uniform contour sampling along the snake, we propose an implicit technique for the resampling of contours. For the application at hand this is suitable as the target shape for the snake is approximately circular. So we introduce another term in the energy functional that makes a snaxel maintain equal distance from its immediate left and right neighboring snaxels. The advantage of such a technique is avoiding the O(*n*) explicit resampling.

If the snaxels are on a circular contour, then the i^{th} and $(i+1)^{th}$ snaxel maintain the following relationships:

$$x_i - x_{i+1} = \bar{R}\cos(\frac{2\pi i}{n}) - \bar{R}\cos(\frac{2\pi(i+1)}{n}),$$
$$y_i - y_{i+1} = \bar{R}\sin(\frac{2\pi i}{n}) - \bar{R}\sin(\frac{2\pi(i+1)}{n}), \quad i = 0,\ldots,n-1, \quad (15)$$

where $\bar{R}$ is the average radius of the snake, as already defined in (11), here to impose cyclic order we note that $x_n=x_0$ and $y_n=y_0$. We now introduce the following energy functional for resampling:

$$E_{\text{sampling}} = \frac{1}{2}\sum_{i=0}^{n-1}\left(x_i - x_{i+1} - d_i^x\right)^2 + \left(y_i - y_{i+1} - d_i^y\right)^2, \quad (16)$$

where the vectors d_i^x and d_i^y are the shorthand notations for the right hand sides of the equations (15). Equation (16) can be written in the following matrix-vector form:

$$E_{\text{sampling}} = \frac{1}{2}\mathbf{x}^T H\mathbf{x} + \frac{1}{2}\mathbf{y}^T H\mathbf{y} - \mathbf{x}^T G\mathbf{d}^{\mathbf{x}} - \mathbf{y}^T G\mathbf{d}^{\mathbf{y}} + \frac{1}{2}(\mathbf{d}^{\mathbf{x}})^T\mathbf{d}^{\mathbf{x}} + \frac{1}{2}(\mathbf{d}^{\mathbf{y}})^T\mathbf{d}^{\mathbf{y}}, \quad (17)$$

where $\mathbf{d}^{\mathbf{x}}$ and $\mathbf{d}^{\mathbf{y}}$ are defined as follows:

$$\mathbf{d}^{\mathbf{x}} = [d_0^x, d_1^x, \ldots, d_{n-1}^x]^T \text{ and } \mathbf{d}^{\mathbf{y}} = [d_0^y, d_1^y, \ldots, d_{n-1}^y]^T \quad (18)$$

and H and G are *n*-by-*n* matrices as follows:

$$H = \begin{bmatrix} 2 & -1 & & & -1 \\ -1 & 2 & -1 & & \\ & \ddots & \ddots & \ddots & \\ & & -1 & 2 & -1 \\ -1 & & & -1 & 2 \end{bmatrix}, \text{ and } G = \begin{bmatrix} 1 & & & & -1 \\ -1 & 1 & & & \\ & \ddots & \ddots & \ddots & \\ & & -1 & 1 & \\ & & & -1 & 1 \end{bmatrix}. \quad (19)$$

The energy is in the quadratic form, so one can now easily obtain the gradient of the energy functional from (17) as:

$$\nabla E_{\text{sampling}} = \left(\frac{\partial}{\partial\mathbf{x}}, \frac{\partial}{\partial\mathbf{y}}\right)E_{\text{sampling}} = \left(H\mathbf{x} - G\mathbf{d}^{\mathbf{x}}, H\mathbf{y} - G\mathbf{d}^{\mathbf{y}}\right). \quad (20)$$

7. Snake Model for Tracking

Having defined the enhancement on GVF, and shape-size and implicit resampling constraints, we are in a position to finally define our proposed snake model to track leukocytes *in vivo*. The proposed snake model is merely the integration of all of the techniques defined above. The snake model is now an approximately circular contour trying to minimize the following energy functional:

$$E_{\text{snake}} = \lambda_1 E_{\text{shape}} + \lambda_2 E_{\text{size}} + \lambda_3 E_{\text{sampling}} + E_{\text{external}} \quad (21)$$

where λ's balance the contribution of different energy functionals. E_{external} is the energy contribution from the enhanced GVF force. Minimization of (21) collects all the relevant Euler equations (13), (14) and (20) and leads to the following discrete from:

$$\lambda_1(\mathbf{x} - \bar{\mathbf{x}} - \bar{R}\mathbf{c}) + \lambda_2(\bar{R} - K)\mathbf{x}_{\mathbf{r}} + \lambda_3(H\mathbf{x} - G\mathbf{d}^x) - \mathbf{f}_{\mathbf{x}} = \mathbf{0} \quad (22)$$

and

$$\lambda_1(\mathbf{y} - \bar{\mathbf{y}} - \bar{R}\mathbf{s}) + \lambda_2(\bar{R} - K)\mathbf{y}_{\mathbf{r}} + \lambda_3(H\mathbf{y} - G\mathbf{d}^{\mathbf{y}}) - \mathbf{f}_{\mathbf{y}} = \mathbf{0} \quad (23)$$

where,

$$\mathbf{f}_{\mathbf{x}} = [u(x_0, y_0), \ldots, u(x_{n-1}, y_{n-1})]^{\mathrm{T}},$$

$$\mathbf{f}_{\mathbf{y}} = [v(x_0, y_0), \ldots, v(x_{n-1}, y_{n-1})]^{\mathrm{T}},$$

$$\mathbf{c} = [\cos(\frac{2\pi(0)}{n}), \ldots, \cos(\frac{2\pi i}{n}), \ldots, \cos(\frac{2\pi(n-1)}{n})]^{\mathrm{T}},$$

$$\mathbf{s} = [\sin(\frac{2\pi(0)}{n}), \ldots, \sin(\frac{2\pi i}{n}), \ldots, \sin(\frac{2\pi(n-1)}{n})]^{\mathrm{T}},$$

$$\mathbf{x}_{\mathbf{r}} = [\frac{x_0 - \bar{x}}{r_0}, \ldots, \frac{x_i - \bar{x}}{r_i}, \ldots, \frac{x_{n-1} - \bar{x}}{r_{n-1}}]^{\mathrm{T}},$$

$$\mathbf{y}_{\mathbf{r}} = [\frac{y_0 - \bar{y}}{r_0}, \ldots, \frac{y_i - \bar{y}}{r_i}, \ldots, \frac{y_{n-1} - \bar{y}}{r_{n-1}}]^{\mathrm{T}}, \text{ with}$$

$$\bar{x} = \frac{1}{n}\sum_{i=0}^{n-1} x_i,\ \bar{y} = \frac{1}{n}\sum_{i=0}^{n-1} y_i,$$

$$r_i = \sqrt{(x_i - \bar{x})^2 + (y_i - \bar{y})^2},\ i = 0, \ldots, n-1.$$

Equations (22) and (23) are the discrete versions of the Euler equations from which we finally get the following gradient descent update equations for the snake to capture the cell in a single image frame:

$$\mathbf{x}^{t+1} = Q^{-1}(\frac{1}{\delta t}\mathbf{x}^t + \mathbf{f}_{\mathbf{x}} + \lambda_1(\bar{\mathbf{x}} + \bar{R}\mathbf{c}) - \lambda_2(\bar{R} - K)\mathbf{x}_{\mathbf{r}}^t + \lambda_3 G\mathbf{d}^x), \text{ and}$$

$$\mathbf{y}^{t+1} = Q^{-1}(\frac{1}{\delta t}\mathbf{y}^t + \mathbf{f}_{\mathbf{y}} + \lambda_1(\bar{\mathbf{y}} + \bar{R}\mathbf{s}) - \lambda_2(\bar{R} - K)\mathbf{y}_{\mathbf{r}}^t + \lambda_3 G\mathbf{d}^y) \quad (24)$$

$$\text{where, } Q = (\frac{1}{\delta t}I + \lambda_1 I + \lambda_3 H).$$

In this context, t and t+1 indicate successive iterations for snake update, and δt is the time step. It can be shown that Q is positive definite and hence its inverse exists. Since Q is constant both in terms of its size and its contents, we need to invert this matrix just one time and then use it in (24) for all the frames of the video sequence. To capture the object in a frame by the snake, one starts with an initial snake on the frame and then iterate with (24) until convergence or until some prescribed number of maximum iterations, whichever occurs first. As already discussed, the initial snake is taken as the position of the snake from the previous frame. The user chooses the initial snake position in the first frame. And this is the only user interaction during tracking of leukocytes.

8. Tracking Results

For the tracking experiments we have observed two types of video sequences – those of vessels treated with TNF-α [14] (16 such sequences) and untreated vessels (17 such sequences). In the second set of experiments, the leukocyte velocity is quite high (>100μm/s) and consequently the tracking task is more challenging. Two types of error measures have been considered: *root mean square error* (RMSE) of the tracked cell center positions (in microns) and the *percentage of frames tracked*. If a computed cell center is within one cell radius from the actual cell center (ground truth), then that frame is considered as "tracked." The percentage is computed as the ratio of number of frames tracked to the total number of frames in the sequence. Figures 2a through Figure 2d provide a comparison of the performances of the proposed snake tracker with the correlation [7] and the centroid trackers [6]. The proposed tracker clearly outperforms the standard trackers by a large margin in both RMSE and percentage of frames tracked. Table 1 summarizes the results shown in Figure 2 by providing the average RMSE as well as the percentage of frames tracked in 16 treated and 17 untreated vessel experiments.

9. References

[1] K. Ley, "Leukocyte recruitment as seen by intravital microscopy," In *Physiology of Inflammation*. K. Ley, editor, New York: Oxford University Press, pp. 303-337, 2001.

[2] N. Manjunath, P. Shankar, B. Stockton, P.D. Dubey, J. Lieberman, U.H. von Andrian, "A transgenic mouse model to analyze CD8+ effector T cell differentiation in vivo," In *Proceedings of the National Academy of Sciences USA*, vol. 96, pp. 13932-13937, 1999.

[3] K.E. Norman, G.P. Anderson, H.C. Kolb, K. Ley, B. Ernst, "Sialyl Lewis^x (sLe^x) and an sLe^x mimetic, CGP69669A, disrupt E-selectin-dependent leukocyte rolling in vivo," *Blood*, vol. 91(2), pp. 475-83, 1998.

[4] C. Xu and J.L. Prince, "Snakes, shapes, and gradient vector flow," *IEEE Trans. Image Processing* vol. 7, pp. 359-369, 1998.

[5] C. Xu and J.L. Prince, "Generalized gradient vector flow external force for active contours," *Signal Processing*, vol. 71, pp. 131-139, 1998.

[6] R.N. Ghosh and W.W. Webb, "Automated detection and tracking of individual and clustered cell surface low density lipoprotein receptor molecules," *Biophysical Journal*, vol. 66, pp.1301-1318, 1994.

[7] G.J. Schütz, H. Schindler, and Th. Schmidt, "Single-molecule microscopy on model membranes reveals anomalous diffusion," *Biophysical Journal*, vol. 73, pp.1073-1080, 1997.

[8] M. Kass, A. Witkin and D. Terzopoulos, "Snakes: Active contour models," *Proceedings of First*

International Conference on Computer Vision, pp. 321-331, 1987.

[9] R. Courant and D. Hilbert, *Methods of mathematics physics*, Vol 1, Interscience Publishers, Inc. New York, 1953.

[10] A. Blake and M. Isard, *Active contours: The application of techniques from graphics, vision, control theory and statistics to visual tracking of shapes in motion*, New York: Springer-Verlag, 1998.

[11] N. Ray, S. T. Acton, T. Altes and E. E. de Lange, "MRI ventilation analysis by merging parametric active contours," In the *Proceedings ICIP 2001*, pp.861-864, Thessaloniki, Greece, October, 2001.

[12] C.A. Hall and T.A. Porsching, *Numerical analysis of partial differential equations*. Englewood Cliffs, New Jersey: Prentice Hall, Inc., 1990.

[13] J.L. Troutman, *Variational calculus with elementary convexity*, Springer-Verlag, New York, 1983.

[14] E.J. Kunkel, Jessica L. Dunne and K. Ley, "Leukocytes arrest during cytokine-dependent inflammation *in vivo*," *The Journal of Immunology*, vol. 164, pp.3302-3308, 2000.

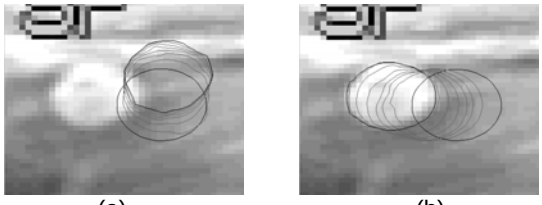

(a) (b)

Figure 1. (a) The standard GVF snake drifts away from the cell; (b) where the improved GVF snake with Dirichlet BC's captures the leukocyte. Initial snake positions are same in both these cases.

Table 1. Average RMSE and percentage of frames tracked.

Experiment	Method	Average RMSE (μm)	Average % Tracked
Treated	Snake	0.5181	99.93
	Correlation	4.87	61.23
	Centroid	6.22	39.01
Untreated	Snake	4.60	74.40
	Correlation	34.25	14.10
	Centroid	33.30	13.07

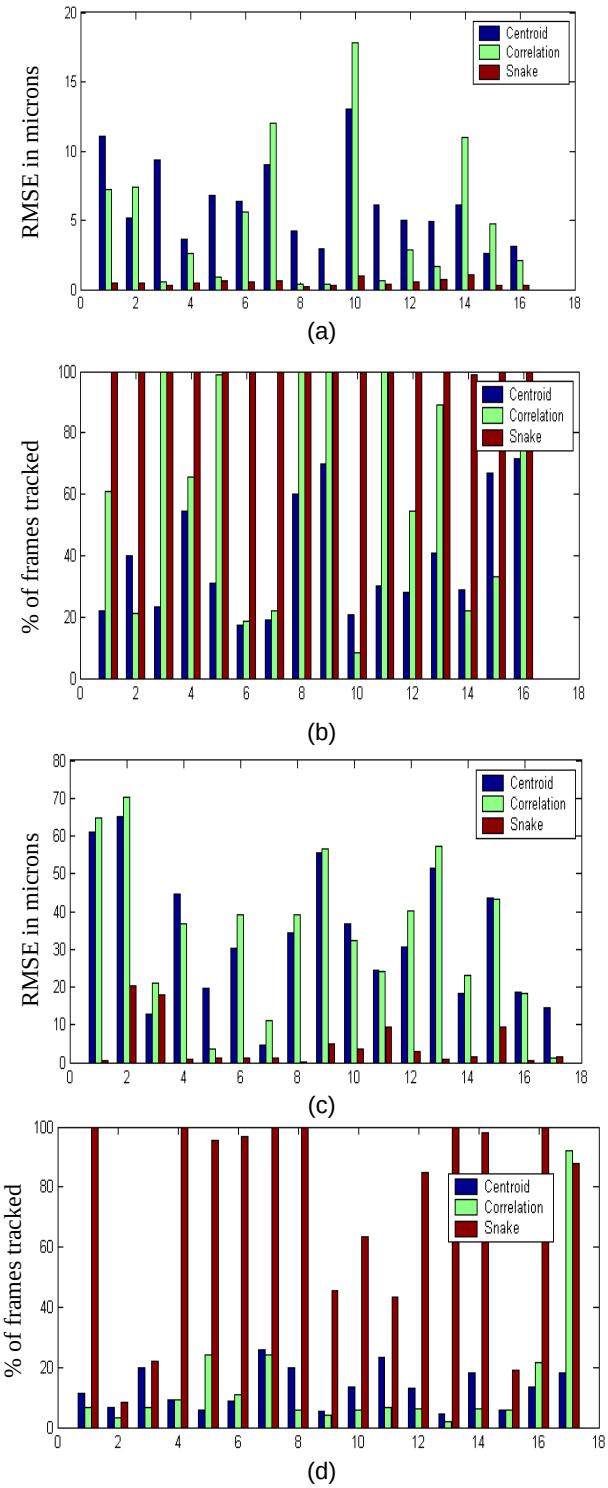

Figure 2. (a) Comparison using the RMSE in cell position in tracking the treated vessel sequences with the three trackers. (b) Comparison using the percentage of frames tracked in the treated sequences. (c) RMSE in tracking untreated sequences with the three trackers. (d) Percentage of frames tracked in untreated sequences with the three trackers. The abscissa provides the sequence number.